Industrial Engineering Journal
ISSN: 0970-2555
Volume : 54, Issue 1, No.4, January : 2025

DESIGN AND ANALYSIS OF MILLING TOOL OPTIMIZATION BY TOPOLOGY TECHNIQUE

V Vashanthan, PG student, Department of Engineering Design,Government College of Technology, Coimbatore, 641 013, Tamilnadu, India. vashanthanvijey153@gmailcom
Dr. N. Nandakumar, Professor, Head of the Department, PG - Engineering Design,Government College of Technology, Coimbatore, 641 013,Tamilnadu, India.
Dr. S. Periyasamy, Associate Professor, Department of PG - Engineering Design,Government College of Technology, Coimbatore, 641 013, Tamilnadu, India.

ABSTRACT
The weight of the milling tool has a significant impact on the mandrel's motion speed during milling operations, particularly when a complicated tool path needs to be followed. Therefore, it is imperative to develop lighter tools without sacrificing mechanical or production performance. Traditionally, the design of a new milling tool cannot be overly complicated due to the limitations of existing manufacturing techniques, which means that it cannot fully achieve the aforementioned criteria. These days, more complicated part geometries may be realized to create lighter, higher-performing tools, due to additive manufacturing (AM) technologies like selective laser melting (SLM) and the topology optimization process. A novel milling tool design with a 30% weight reduction is given in this study; the SLM method has been chosen to make the milling tool a reality. The revised geometry has been slightly altered to reduce the amount of support structures needed to accurately materialize the intended component, which are necessary for the SLM process. All of the component's support structures have been successfully eliminated, and a lighter milling tool has been created.
Keywords: Milling Tool, Additive Manufacturing, Selective Laser Melting

I.Introduction
The processes that create components by layers on material are referred to as additive manufacturing (AM) technology. In collaboration with AM, a set of principles known as "Design for Additive Manufacturing" (DFAM) was created to help designers maximize the potential of these technologies. Depending on the procedure used, these technologies can be used in a variety of contexts because of the AM's special characteristics. Even the tools used in manufacturing processes may be rethought with AM. The weight of the milling tool has a significant impact on the mandrel's motion speed these days, particularly when a complicated tool path needs to be followed. Lighter tools must thus be developed without significantly lowering mechanical or manufacturing performance. The design of a milling tool is restricted to the intricacy of the exterior shape due to the limitations of standard production procedures; nevertheless, only complete pieces can be created in the cross section. More complicated component geometries may be realized and more lightweight, high-performance tools can be obtained thanks to the AM procedures and the topology optimization approach.
However, the normal limitations of AM technologies are not included in the topology optimization. By including the restrictions of AM processes into their optimization approach, the researchers attempted to address this issue. To minimize the need of support structures in the component's implementation, the topology optimization has, for instance, utilized the maximum printed overhang angle [1–3]. Additionally, unfused powder or support structure material should be able to be evacuated from the interior parts of a 3D printed product. In order to prevent enclosed voids in the part's structure, the LI QH et al. [4] study attempted to add a connection restriction to the topology optimization approach.
The researchers tried to solve this problem by incorporating the limitations of AM techniques into their optimization strategy. For example, the topology optimization has used the maximum printed overhang angle to reduce the requirement for support structures in the construction of the component

Industrial Engineering Journal
ISSN: 0970-2555
Volume : 54, Issue 1, No.4, January : 2025

[1–3]. A 3D printed product should also have the ability to remove unfused powder or support structure material from its inner sections. The topology optimization method to avoid enclosed voids in the part's construction.

II.Materials and methods

The redesign of a milling tool, mostly utilized in face milling operations, was the aim of this study.

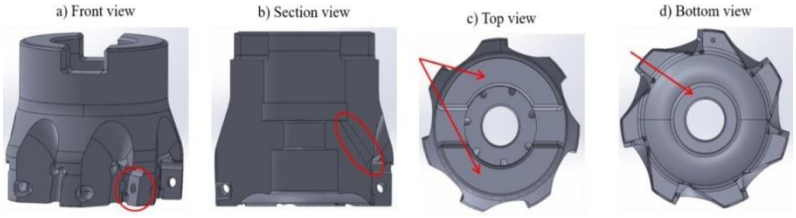

Figure 1: shows the milling tool's shape and key characteristics.

One of the seven insert places is highlighted by the red circle in figure 1a. The refrigerant fluid channel is seen in Figure 1b, and the arrows in Figure 1c indicate the surfaces that match between the mandrel and the milling tool. A screw that matches the surface of the component under study. The redesign of the milling tool has been reached through two steps:

• Reduction of the support structures needed for the SLM process;
• Optimization of the original milling tool's topology.

The best redistribution of the material within a constrained design space is the primary objective of topology optimization, a structural optimization. Knowing which areas of the milling tool were most affected by loads and deformations was crucial to achieving an accurate optimization. As a result, the component has undergone a static analysis. Altair Inspire was the program used to do this. The model set-up of the static analysis consists of an assembly composed by the milling tool, seven inserts, the screws required to fix the inserts, seven cutting forces (the red arrows) and the supports applied to the model. Table 2 contains the values of the parameters selected to estimate the cutting force Ft, according to the specific cutting pressure model (ks0 model) [5]. This load was applied to every insert and acted on the red surface (4 mm length and 0,16 mm width) of figure 2a.

Table 1: parameters used to estimate the cutting force

PARAMETER	VALUE
Cutting edge angle β	92
Load fracture (MPa)	1250
Z coefficient	0.197
Milling width dr	D3
Feed for tooth (mm)	0.16
Depth of cut (mm)	4
Number of teeth Z	7

Every cutting force was characterized by a direction perpendicular to a plane that connects the centre of the milling tool and the extremity of the insert where the force was applied (figure 2b).

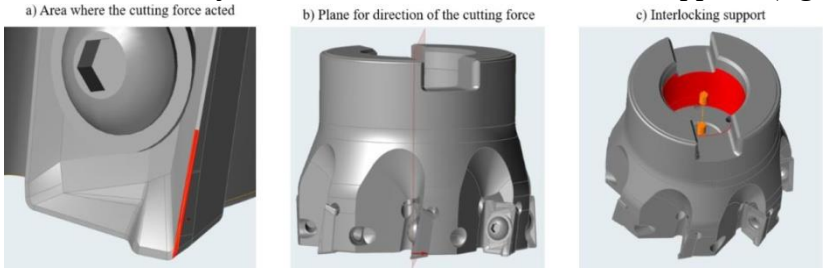

Figure 2: a) application area of the cutting force; b) plane used for the direction of the cutting force; c) interlocking support.

Since there was limited space for relative movement between the mandrel and the milling tool, an interlocking support was used to approximate the junction between the two components on the red surfaces in figure 2c. The screws used to secure the inserts were subjected to a pretension of 2400 N. The 1.2344 alloy steel, whose mechanical characteristics are displayed in table 2, was the material utilized for the simulation. These characteristics were discovered in books.

Table 2: 1.2344 mechanical properties .

	DENSITY(g/cm^3)	YIELD STRENGTH (MPa)	YOUNG MODULUS E (GPa)
1.2344 steel	7.9	920	210

The design space selected for the topological optimizations is indicated by the brown surfaces in figure 3. Each component inside this space may be optimized and modified, but the rest had to keep their original shape. The matching surface between the mandrel and the milling tool, the screw hole connecting these two parts (figure 3b), the screw holes for the inserts, the surfaces where the interlocking support was placed, and the seven inserts were not included in the design area.

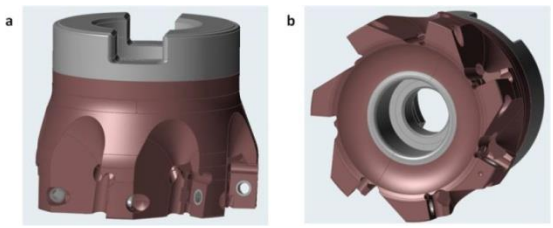

Figure 3: a) design space set for the topology optimization; b) hole for the screw of the mandrel.

For the topology optimization in this study, two primary constraints have been established: maximizing stiffness and reducing the mass of the design space by 70%. The topology optimization produced a raw geometry that has to be softened because of its operating principles. The 3DExpert program has been used to examine the smoothed geometry and determine which regions require support structures. These structures were necessary for down-facing surfaces wider than 2 mm and overhanging surfaces with a slope less than 30° from the horizontal direction, per the software's established requirements (figure 4). The support structures greatly affect the time needed for the post processing phase. Moreover, if these elements are needed in the internal surfaces of the milling tool they are hardly accessible or totally unreachable, so they can not be removed. Thus, to minimize the use of the support structures, small changes in the smoothed geometries have been made so that there were no areas with the characteristics shown in figure 5. All these changes will be discussed in detail in the next sections.

In order to verify the mechanical performance of the new geometry, a static analysis has been performed with the same model set-up shown in figure 2. To check the geometry printability, the part was produced through the SLM process and the 17-4 PH was selected as material. Table 3 resumes the powder mechanical properties.

Table 3:17-4PH mechanical properties

	DENSITY(g/cm^3)	YIELD STRENGTH (MPa)	YOUNG MODULUS E (GPa)
17-4PH steel	7.75	1100	197

Industrial Engineering Journal
ISSN: 0970-2555
Volume : 54, Issue 1, No.4, January : 2025

III.Results

Static analysis of the traditional geometry

The displacement map in figure 5 shows that the areas closest to the mandrel and milling tool matching surfaces experience the least amount of movement. In fact, the examined component was severely constrained by a series of interlocking limitations. Because of the cutting forces acting there, the insert positions showed the largest displacements.

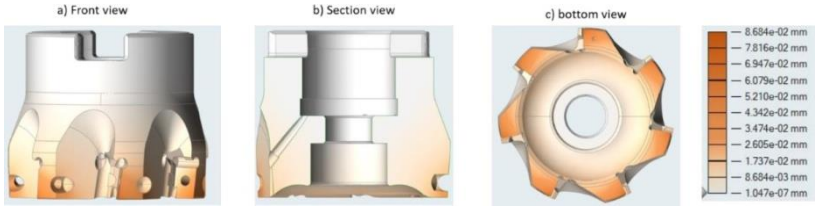

Figure 5: map of displacements of the traditional milling tool geometry.

The maps of the Von Mises stress shows that the contact areas between the milling tool and the inserts are subjected to the highest stress, proving that the locations of the inserts are the most stressed areas of the component.

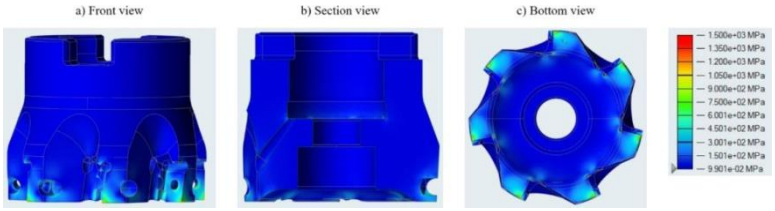

Figure 6: maps of the Von Mises stress of the traditional milling tool geometry

Optimization of topology and smoothed geometry

Figure 7 displays the outcomes of the topology optimization. The optimization redistributed the material within the design space, as shown by the brown surfaces. It is evident that this raw geometry could not be printed owing to the significant surface roughness, a lot of sharp edges created by the optimization and the low dimensional accuracy.

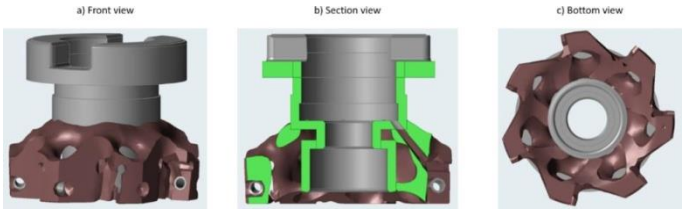

Figure 7: topology optimization results. The brown surfaces represent the optimal distribution of the material according to the topology optimization.

The CAD program Solidworks has been used to modify the conventional milling tool in order to get a geometry free of these flaws. A new milling tool design has been created based on the form that the topology optimization recommended. The revised smoothed geometry is seen in Figure 8.

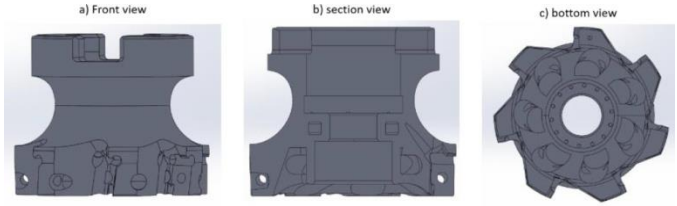

Figure 8: smoothed geometry of the milling tool.

Minimization of Support structures

Every modification made to the smoothed geometry to reduce the support structures is displayed in the following images. The places where the supports were required are shown by the blue and yellow patches.

Industrial Engineering Journal
ISSN: 0970-2555
Volume : 54, Issue 1, No.4, January : 2025

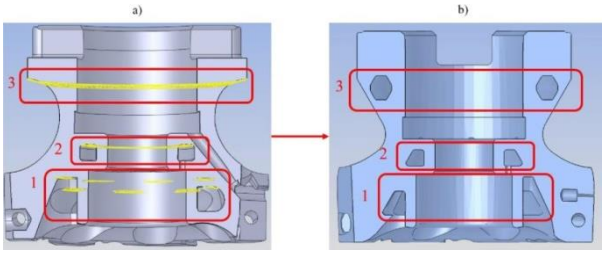

Figure 9: section view of the milling tool before and after the geometry adjustment.
a) Section view before geometry adjustment; b) section after the adjustments.

The yellow areas in figures 9a inside red box 1 have been transformed into trapezoids (figure 9b). Because of this modification, these portions' downfacing surfaces were less than 2 mm broad, negating the need for supports. within these interior areas. The rectangular channel within red box 2 then become trapezoidal, eliminating the requirement for the supports (figure 9b). Lastly, the milling tool contour change shown in figure 9a is displayed in box 3 of figure 9b. An internal channel that lowers the tool's overall weight was made possible by this modification. The octagonal design made it possible to provide this element without the need for supports. To evacuate the powder from this channel, six holes were created (Figure 10a). However, the circular shape required support structures, thus the holes assumed an elliptical geometry (Figure 10b).

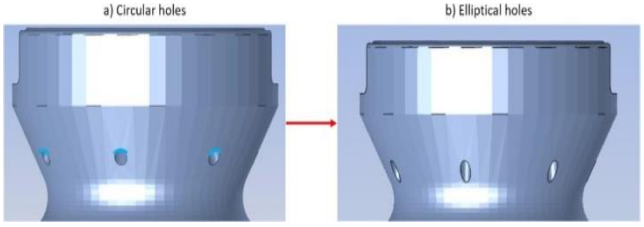

Figure 10: adjustment of the holes used to evacuate the powder.

Since the circular channels for the refrigerant fluid needed support structures (red circle of figure 11a), their shape has been turned into dog bone ones (figure 11b).

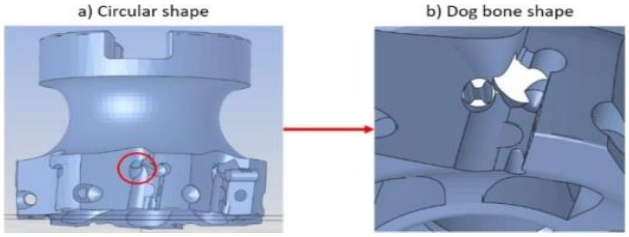

Figure 11: geometry adjustment of the channel for the refrigerant fluid.

While the extensions of the surfaces in figure 12d decrease the curvature radius of the regions underlined by the red circles in figure 12c and make these parts of the tool self-supporting, the surfaces highlighted in figure 12a have been altered to reach an octagonal shape (figure 12b) and avoid the use of supports in these areas.

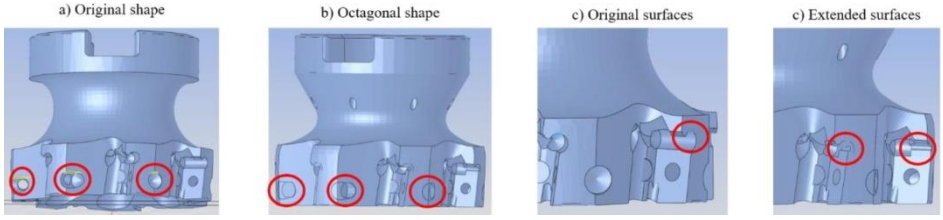

Figure 12: geometry changes in the locations for inserts.

An outline of the support structures needed by the milling tool during the "smoothing phase" and following the geometry changes is shown in Figure 13. While the section view of figure 13b demonstrates that the use of these structures has been restricted to separating the milling tool from the 3D printer's baseplate and maintaining the matching surface between the milling tool and the screw for the mandrel, the front view of figure 13a reveals the smoothed geometry required much

more supports.

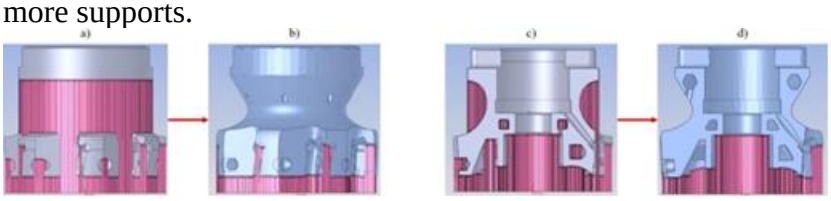

Figure 13: comparison of the two milling tool geometry
a) Front view of the smoothed geometry; b) front view of the adjusted geometry; c) section view of the smoothed geometry; d) section view of the adjusted geometry

Traditional geometry vs Redesign geometry

Figure 14 and Table 4 display the new milling tool's mechanical performance. The displacement and Von Mises stress maps demonstrate that, despite the milling tool's altered form, its behavior remained unchanged: the inserts' locations are the most stressed and move the most.

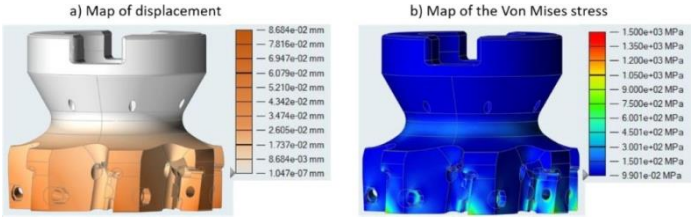

Figure 14: map of displacement and Von Mises stress for the redesign milling tool

Mechanical Performance Comparison

	DISPLACEMENT (mm)	MAXIMUM VON MISSES STRESS (Mpa)	MASS (Kg)
Original Geometry	0.04297	1200	0.295
New Design Geometry	0.08361	1400	0.209
Percentage Increases	94.6%	16.7%	-29.2%

Although the maximum displacement became two times greater, its absolute value was still small while the maximum Von Mises stress has been increased of 16,7%. Thus the mechanical performances of the new geometry are similar to the traditional milling tool, despite a 30% reduction of the mass.

IV. Conclusion

The topology optimization approach has been used to build a new geometry for the milling tool. Although the revised shape is 30% lighter, it experiences a greater maximum stress (about 17%). The twofold displacement (from 0.04 to 0.08 mm) that is still suitable for the machining environment is the source of the greater performance drop that is noted. Furthermore, fewer support structures are required now that the geometries have been adjusted. In fact, the new design features a support structure that is perpendicular to the base plate just to keep the matching surface between the milling tool and the mandrel screw in place and to detach the tool from the plate.

References

[1]Qian X. Undercut and overhang angle control in topology optimization: a density gradient based integral approach. Int J Numer Methods Eng2017; 111:247–72.

[2]Allaire G, Dapogny C, Estevez R, Faure A, Michailidis G. Structural optimization under overhang constraints imposed by additive manufacturing technologies. J Comput Phys 2017; 351:295–328.

[3]Guo X, Zhou JH, Zhang WS, Du ZL, Liu C, Liu Y. "Self-supporting structure design in additive manufacturing through explicit topology optimization". Comput Methods Appl Mech Engrg 2017; 323:27–63.

[4]Li QH, Chen WJ, Liu S, Tong LY. "Structural topology optimization considering connectivity constraint". Struct Multidiscip Optim 2016; 54(4):971–84.

[5]Monroy Vazquez K.P., Giardini C., Ceretti E. (2014) Cutting Force Modeling. In: The International Academy for Production Engineering, Laperrière L., Reinhart G. (eds) CIRP Encyclopedia of Production Engineering. Springer, Berlin, Heidelberg. https://doi.org/10.1007/978-3-642-20617-7_6399.

[6]Wang, J., Lin, W., Han, P. & Zhou, Q. 2012, "Failure analysis of H13 steel hot-forging die for earlier damage", Jinshu Rechuli/Heat Treatment of Metals, vol. 37, no. 9, pp. 122-124.